A Novel Rigid β-Turn Molecular Scaffold

Angela Lombardi,[†] Gabriella D'Auria,[†] Ornella Maglio,[‡] Flavia Nastri,[‡] Laura Quartara,[§] Carlo Pedone,[‡] and Vincenzo Pavone*,[†]

Contribution from the Centro Interuniversitario di Ricerca su Peptidi Bioattivi, University of Naples "Federico II", Via Mezzocannone 4, I-80134 Napoli, Italy, Centro diStudio di Biocristallografia-CNR, Via Mezzocannone 4, I-80134 Napoli, Italy, and A. Menarini Pharmaceutical Industries, Via Sette Santi 3, 50131 Firenze, Italy

Received December 17, 1996. Revised Manuscript Received November 25, 1997

Abstract: We describe here the solution ^{1}H NMR analysis, restrained and unrestrained molecular dynamic simulations of the bicyclic peptide *cyclo*(Met^1-asp^2-Trp^3-Phe^4-dap^5-Leu^6)*cyclo*(2β-5β) (MEN10701) (dap: (2*R*)-2,3-diaminopropionic acid). This compound is an analogue of *cyclo*(Met^1-Asp^2-Trp^3-Phe^4-Dap^5-Leu^6)*cyclo*(2β-5β) (MEN10627) (Dap: (2*S*)-2,3-diaminopropionic acid), which is the most potent and selective, peptide-based NK$_2$ receptor antagonist known to date. MEN10701 differs from MEN10627 for the D chirality of the Asp^2 and Dap^5 residues; it was designed to better understand the role of the lactame bridge in determining the shape of the molecule and to elucidate whether its position, above or below the plane containing the pharmacophores (Met^1, Trp^3, Phe^4, and Leu^6 side chains), could modulate the biological response. Despite our expectations, the uncoercible bicyclic structure of MEN10627 is dramatically coerced into a novel conformation, by the replacement of the lactame bridge forming units (Asp^2 and Dap^5) with residues of opposite chirality. The overall shape of MEN10701 is also quite unique because of its compactness. It is ellipsoidal instead of being rectangle-like, and the structure is stabilized by two *intra*molecular hydrogen bonds encompassing two type I′ β-turns. This structure can be added to the repertoire of rigid β-turn scaffolds for the design of bioactive molecules, which require turned motifs to elicit potency and specificity.

Introduction

Cyclic peptides represent useful model systems to study the propensity of α-amino acids to be accommodated within turned structure. They can also provide template structures for the design of new bioactive peptides. Cyclization of the N- and C-terminal ends of linear bioactive peptides is often performed with the aim of reducing the conformational freedom of the parent linear compounds.[1−3] Despite the topological constraint, introduced in the cyclization process, cyclic peptides still possess a remarkable flexibility.[4−12] Cyclic hexapeptides have been studied in detail both in the solid state and in solution, and they often contain two β-turns.[9,10,13−23] They are also characterized by a flat rectangular or twisted-rectangular shape.

A nice example of N- to C-terminal cyclization which leads to a more active analogue is given by NK$_2$ receptor antagonists.[24] L659,877 or *cyclo*(Met^1-Gln^2-Trp^3-Phe^4-Gly^5-Leu^6), is an active product formally derived from head to tail cyclization of the previously reported weak antagonist L659,874 or Ac-Leu-Met-Gln-Trp-Phe-Gly-NH$_2$. The enhancement of antagonist activity and selectivity derived from cyclization, clearly showed that the favorable conformation for specific interaction with NK$_2$

* To whom correspondence should be addressed. Telephone: +39-81-5476550. Fax: +39-81-5527771. E-mail: pavone@chemna.dichi.unina.it.
† University of Naples "Federico II".
‡ Centro di Studio di Biocristallografia-CNR.
§ A. Menarini Pharmaceutical Industries.

(1) Kessler, H. *Angew. Chem., Int. Ed. Engl.* **1982**, *21*, 512−523.
(2) Rizo, J.; Gierasch, L. M. *Annu. Rev. Biochem.* **1992**, *61*, 387−418.
(3) De Grado, W. F. *Adv. Protein Chem.* **1988**, *40*, 51−125.
(4) Karle, I. L.; Karle, J. *Acta Crystallogr.* **1963**, *16*, 969−975.
(5) Gilon, C.; Halle, D.; Chorev, M.; Selinger, Z.; Bik, G. *Biopolymers* **1991**, *31*, 745−750.
(6) Di Blasio, B.; Rossi, F.; Benedetti, E.; Pavone, V.; Pedone, C.; Temussi, P. A.; Zanotti, G.; Tancredi, T. *J. Am. Chem. Soc.* **1989**, *111*, 9089−9098.
(7) Gurrat, M.; Muller, G.; Kessler, H.; Aumailley, M.; Timpl, R., *Eur. J. Biochem.* **1992**, *210*, 911−921.
(8) Di Blasio, B.; Lombardi, A.; D'Auria, G.; Saviano, M.; Isernia, C.; Maglio, O.; Paolillo, L.; Pedone, C.; Pavone, V. *Biopolymers* **1993**, *33*, 621−631.
(9) Pavone, V.; Lombardi, A.; Saviano, M.; Di Blasio, B.; Nastri, F.; Fattorusso, R.; Maglio, O.; Isernia, C. *Biopolymers* **1994**, *34*, 1505−1515.
(10) Pavone, V.; Lombardi, A.; Saviano, M.; Nastri, F.; Fattorusso, R.; Maglio, O.; Isernia, C.; Paolillo, L.; Pedone C. *Biopolymers* **1994**, *34*, 1517−1526.
(11) Lombardi, A.; Saviano, M.; Nastri, F.; Maglio, O.; Mazzeo, M.; Pedone, C.; Isernia, C.; Pavone, V. *Biopolymers* **1996**, *38*, 683−691.
(12) Lombardi, A.; Saviano, M.; Nastri, F.; Maglio, O.; Mazzeo, M.; Isernia, C.; Paolillo, L.; Pavone, V. *Biopolymers* **1996**, *38*, 693−703.
(13) Smith, J. A.; Pease, L. G. *CRC Crit. Rev. Biochem.* **1980**, *8*, 315−399.
(14) Karle, I. L. in *Peptides*; E. Gross and J. Meinhofer, Eds.; Academic Press: New York; 1981, Vol. 4, pp 1−54 and references therein.
(15) Ovchinnikov, Yu V.; Ivanov, V. T. In *Proteins*; Neurath, H., Hill, R. L., Eds.; Academic Press: New York, 1982; Vol. 5, pp 307−341.
(16) Gierasch, L. M.; Rockwell, A. L.; Thompson, K. F.; Briggs, M. S. *Biopolymers* **1985**, *24*, 117−135.
(17) Rose, G. D.; Gierasch, L. M.; Smith, J. A. In *Advances in Protein Chemistry*; Anfinsen, C. B., Edsall, J. T., Richards, F. M., Eds.; Academic Press: Orlando, FL, 1985; Vol. 37, pp 1−109.
(18) Paul, P. K. C.; Ramakrishanan, C. *Int. J. Pept. Protein Res.* **1987**, *29*, 433−454 and references therein.
(19) Kessler, H.; Haupt, A.; Schudok, M.; Ziegler, K.; Frimmer, M. *Int. J. Pept. Protein Res.* **1988**, *32*, 183−193.
(20) Bean, J. W.; Kopple, K. D.; Peishoff, C. E. *J. Am. Chem. Soc.* **1992**, *114*, 5328−5334.
(21) Prachand, M. S.; Singh, S.; Dhingra, M. M.; Singh, U.; Ghosh, S. K., Mamdapur, V. R.; Chandha, M. S. *Magn. Reson. Chem.* **1993**, *31*, 944−953.
(22) Kessler, H.; Matter, H.; Gemmecker, G.; Diel, H. J.; Isernia, C.; Mronga, S. *Int. J. Pept. Protein Res.* **1994**, *43*, 47−61.
(23) Matter, H.; Kessler, H. *J. Am. Chem. Soc.* **1995**, *117*, 3347−3359.
(24) McKnight, A. T.; Maguire, J. J.; Elliot, N. J.; Fletcher, A. E.; Foster, R.; Tridgett, R.; Williams, J.; Longmore, J.; Icersen, L. L. *Br. J. Pharmacol.* **1991**, *104*, 355−360.

S0002-7863(96)04332-6 CCC: $15.00
Published on Web 06/05/1998

receptor was mimicked. However, L659,877 still possesses a considerable conformational flexibility in solution, as ascertained by NMR analysis.[25−28] A further improvement was achieved by us with a more constrained analogue whose backbone could adopt a unique backbone conformation. A second cyclization through β functional groups inserted at positions 2 and 5 of L659,877 was performed, yielding the bicyclic peptide *cyclo*(Met^1-Asp^2-Trp^3-Phe^4-Dap^5-Leu^6)*cyclo*(2β-5β) (Dap: (2*S*)-2,3-diaminopropionic acid), named MEN10627.[29−31] This bicyclic peptide is the most potent NK_2 receptor antagonist described to date; it possesses high affinity for the NK_2 receptor, 10−100 fold higher than the parent monocyclic compound at the NK_2 receptor expressed in different species.[30] The potency, specificity of action, and long-lasting activity *in vivo* of MEN10627 is strikingly related to its well-defined three-dimensional structure and to its rigid conformation in solution. The structure of MEN10627, both in solution and in the solid state, is defined by a type I and a type II β-turn, with Trp^3-Phe^4 and Leu^6-Met^1 as corner residues, respectively. This conformation is further stabilized by two *intra*molecular hydrogen bonds between the C′O and NH groups of Asp^2 and Dap.^{5} We demonstrated that the bicyclic structure of MEN10627 and of its analogue *cyclo*(Phe^1-Asp^2-Trp^3-Phe^4-Dap^5-Trp^6)*cyclo*(2β-5β)[32] are quite rigid, and thus this bicyclic structure was recently proposed as a general type I/type II β-turn molecular scaffold for the design of bioactive molecules which require turned motifs to elicit potency and specificity.[32]

In this paper we report the conformational analysis, carried out in CD_3CN solution by NMR spectroscopy, of *cyclo*(Met^1-asp^2-Trp^3-Phe^4-dap^5-Leu^6)*cyclo*(2β-5β) (MEN10701) (dap: (2*R*)-2,3-diaminopropionic acid). Restrained molecular dynamic (RMD) simulation and unrestrained molecular dynamic (MD) simulation *in vacuo* were also performed to build refined molecular models and to evaluate the rigidity of MEN10701. This bicyclic peptide differs from the parent compound MEN10627 for the D chirality of the Asp^2 and Dap^5 residues. MEN10701 was designed to better understand the role of the lactame bridge in modulating the biological response. In our initial hypothesis, the molecular structure of MEN10701 would be characterized by a relative orientation of the pharmacophores (Trp, Phe, Leu, and Met side chains) similar to that found in MEN10627, but with a different position of the lactame bridge. We demonstrate here that the replacement of the lactame bridge forming units (Asp^2 and Dap^5) with residues of opposite chirality coerces the peptide scaffold to adopt a conformation quite different from that found for MEN10627. As a consequence, a dramatic drop in biological activity is observed.[33] We propose here that the bicyclic structure of MEN10701 can be used as a novel rigid scaffold for the design of type I′ β-turned conformation.

Experimental Section

Materials. MEN10701 was synthesized as previously described[29,32] and provided by Laura Quartara. CD_3CN (100% relative isotopic abundance) was from Cambridge Isotope Laboratories, Inc.; TMS (tetramethylsilane) was from Aldrich.

NMR Analysis. ^{1}H NMR 1D and 2D experiments were performed on a VARIAN UNITY 400 spectrometer, operating at 400 MHz. VNMRS 4.3 software (Varian Associates Inc., Palo Alto, CA) was used for free induction decay acquisitions and data processing, on a SUN SPARC Station 1+, located at the "Centro Interuniversitario di Ricerca su Peptidi Bioattivi", University of Naples "Federico II".

All NMR spectra of MEN10701 were recorded at 298 K from a 2.4 mM CD_3CN solution, using TMS as internal standard. Spin system assignments were made by using a combination of scalar and dipolar correlation 2D experiments.[34] Phase-sensitive double-quantum filtered correlated spectroscopy (DQF−COSY),[35] total correlation spectroscopy (TOCSY),[36] nuclear Overhauser enhancement spectroscopy (NOESY),[37] and exclusive COSY (E-COSY)[38] were performed according to the States−Haberkorn method.[39] Typically 4096 complex time domain data points were acquired in F2 over 4000 Hz of spectral width. Two times 256 increments were accumulated in F1 using 40 transients for every t1 increment. The data matrix was zero filled to 1K × 4K and multiplied by sine−bell functions prior to Fourier transformations. TOCSY experiment was carried out using 70 ms MLEV-17 spin lock (field strength 10 kHz).[36] NOESY experiments were acquired at 100, 150, and 300 ms. Integrations of NOESY peaks were performed using the available Varian software. The NOESY experiments yielded 64 NOE contacts in positive regime. Cross relaxation rates for each spin pair were obtained by the initial build-up rate approximation.[40] The Trp^3 $\beta,\beta'CH_2$ distance of 1.78 Å was used as a reference distance. ^3J coupling constant values were obtained from 1D and from E-COSY spectra. The prochiral assignments were achieved for $\beta,\beta'CH_2$ protons of asp^2 and Trp^3 residues, according to their $^3J_{\alpha CH-\beta(\beta')CH}$ coupling constants and NH-$\beta(\beta')$CH, αCH-$\beta(\beta')$CH NOESY cross-peak intensities.[41] For these residues it was possible to calculate the populations of their side chains χ^1 rotamers, by following previously described methods.[42,43] Stereospecific assignments was not achieved for $\beta,\beta'CH_2$ protons of the remaining residues due to (i) overlapping β-proton resonances of dap^5, (ii) lack of measurable NH−$\beta(\beta')$CH, NOESY cross-peaks for Met^1, (iii) lack of measurable NH−$\beta(\beta')$CH, αCH−$\beta(\beta')$CH NOESY cross-peaks for Phe^4, and (iv) $^3J_{\alpha CH-\beta(\beta')CH}$ coupling constant values for Leu^6 (see Table 1). The temperature coefficients of amide protons were obtained from 1D and, when necessary, from 1D TOCSY spectra[44] at different temperatures. The proton chemical shifts, coupling constants, and temperature gradients of amide protons are reported in Table 1. Notable *inter*proton distances calculated from NOE connectivities are listed in Table 2.

(25) Wolborn, U.; Brunne, R. M.; Hartinh, J.; Holzemann, G.; Leibfritz, D. *Int. J. Pept. Protein Res.* **1993**, *41*, 376−384.

(26) Siahaan, T. J.; Lutz, K. *J. Pharmacol. Biomed. Anal.* **1994**, *12*, 65−71.

(27) Zhang, M.; Quinn, T. P.; Wong, T. C. *Biopolymers* **1994**, *34*, 1165−1173.

(28) Amodeo, P.; Rovero, P.; Saviano, G.; Temussi, P. A. *Int. J. Pept. Protein Res.* **1994**, *44*, 556−561.

(29) Pavone, V.; Lombardi, A.; Nastri, F.; Saviano, M.; Maglio, O.; D'Auria, G.; Quartara, L.; Maggi, C. A.; Pedone, C. *J. Chem. Soc., Perkin Trans. 2* **1995**, 987−993.

(30) Pavone, V.; Lombardi, A.; Maggi, C. A.; Quartara, L.; Pedone, C. *J. Pept. Sci.* **1995**, *1*, 236−240.

(31) Quartara, L.; Pavone, V.; Pedone, C.; Lombardi, A.; Renzetti, A. R.; Maggi, C. A. *Regul. Pept.* **1996**, *65*, 55−59.

(32) Lombardi, A.; D'Auria, G.; Saviano, M.; Maglio, O.; Nastri, F.; Quartara, L.; Pedone, C.; Pavone, V. *Biopolymers* **1996**, *40*, 505−518.

(33) Quartara, L.; Fabbri, G.; Patacchini, R.; Maggi, C. A.; Astolfi, M.; D'Auria, G.; Maglio, O.; Lombardi, A.; Pedone, C.; Pavone, V. *Peptides 1994*; Maia, H. L. S. Ed, Escom: Leiden, The Netherlands, 1995; pp 591−592.

(34) Wuthrich, K. *NMR of Proteins and Nucleic Acids*; Wiley: New York, 1986.

(35) Piantini, U.; Sørensen, O. W.; Ernst, R. R. *J. Chem. Phys.* **1982**, *104*, 6800−6801.

(36) Bax, A.; Davis, D. G. *J. Magn. Reson.* **1985**, *65*, 355−360.

(37) Jeener, J.; Meier, B. H.; Bachman, P.; Ernst, R. R. *J. Chem. Phys.* **1979**, *71*, 4546-4553.

(38) Griesinger, C.; Ernst, R. R. *J. Magn. Reson.* **1987**, *75*, 261−271.

(39) States, D. J.; Haberkorn, R. A.; Ruben D. J. *J. Magn. Reson.* **1982**, *48*, 286−292.

(40) Neuhaus, D.; Williamson, M. *The Nuclear Overhauser Effect in Structural and Conformational Analysis*; VCH Publishers Inc.: New York, 1989.

(41) Clore, G. M.; Gronenborg, A. M. *Crit. Rev. Biochem. Mol. Biol.* **1989**, *24*, 479−563.

(42) Jardetzky, O.; Roberts, G. C. K. In *NMR in Molecular Biology*; Academic Press Inc.: New York, 1981; pp 115−186.

(43) Kessler, H.; Griesinger, C.; Wagner, K. *J. Am. Chem. Soc.* **1987**, *109*, 6927−6933.

(44) Kessler, H.; Anders, U.; Gemmecher, G.; Steuernagel, S. *J. Magn. Reson*. **1989**, *85*, 1−14.

Table 1. Proton Chemical Shifts, ^3J Coupling Constants, and Temperature Coefficients of *Cyclo*(Met[1]-asp[2]-Trp[3]-Phe[4]-dap[5]-Leu[6])-*Cyclo*(2β-5β), in CD_3CN, at 298 K[a]

residue	proton	δ (ppm)	^3J (Hz)	$-\Delta\delta_{NH}/\Delta T$(ppb/K)
Met[1]	NH	7.88	J(NH−αCH) = 5.4	8.2
	αCH	3.85	J(αCH−βCH) = 4.3	
	βCH	2.35	J(αCH−β'CH) = 10.1	
	β'CH	2.20		
	γCH	2.65		
	γ'CH	2.52		
	SCH_3	2.07		
asp[2]	NH	6.47	J(NH−αCH) = 6.5	3.2
	αCH	4.40	J(αCH−βCHpro*R*) = 4.2	
	βCHpro*R*	2.53	J(αCH−βCHpro*S*) = 4.2	
	βCHpro*S*	2.18		
Trp[3]	NH	7.18	J(NH−αCH) = 9.8	1.7
	αCH	4.82	J(αCH−βCHpro*S*) = 10.1	
	βCHpro*S*	3.41	J(αCH−βCHpro*R*) = 5.4	
	βCHpro*R*	2.84		
	2H	7.2		
	4H	7.68		
	5H	7.05		
	6H	7.15		
	7H	7.45		
	ϵNH	9.20		
Phe[4]	NH	7.64	J(NH−αCH) = 6.6	3.2
	αCH	3.55	J(αCH−βCH) = 2.8	
	βCH	3.18	J(αCH−β'CH) = 11.3	
	β'CH	2.66		
	2,6H	6.38		
	3,5H	6.98		
	4H	- - -		
dap[5]	NH	8.28	J(NH−αCH) = 5.9	2.4
	αCH	4.25		
	$\beta\,\beta'$CH	3.50		
	βNH	7.38		7.0
Leu[6]	NH	7.74	J(NH−αCH) = 9.2	0.9
	αCH	4.68	J(αCH−βCH) = 7.6	
	βCH	1.90	J(αCH−β'CH) = 7.6	
	β'CH	1.76		
	γCH	1.63		
	δCH_3	1.03		
	$\delta' CH_3$	0.96		

[a] Concentration 2.1 mg/mL. Chemical shifts are referred to TMS.

Computational Details. All the computations were performed using a Silicon Graphics Indigo 2 workstation. The package Insight II/Discover (Biosym Technologies, San Diego, CA)[44] with the consistent valence force field (CVFF)[46−48] was used for energy minimization, RMD, and MD simulations. The starting model was manually built, using the standard bond geometry for amino acid residues supplied with the Biopolymer module of the Insight II program.[43] The peptide backbone, including the lactame bridge, was unequivocally fixed in a reasonable initial conformation by an approximate evaluation of 11 main chain to main chain *inter*-residue NOE derived *inter*proton distances (3 NOEs per residue), all the $^3J_{NH-\alpha CH}$ values and the $^3J_{\alpha CH-\beta(\beta')CH}$ for asp[2], and the temperature coefficients. The only point of ambiguity was due to the $^3J_{\alpha CH-\beta(\beta')CH}$ of dap[5], but the covalent structure of the bicycle left very little margin of uncertainity for the χ^1 angle. Subsequently, side chains were modeled in their dominantly populated conformations. Unambiguous values of $^3J_{\alpha CH-\beta(\beta')CH}$ coupling constants and NH-$\beta(\beta')$CH, αCH-$\beta(\beta')$CH NOESY cross-peak intensities allowed us to define the Trp[3] χ^1 angle. The Trp[3] χ^2 angle was determined by the Trp[3]4H to main-chain *inter*proton distances, derived from NOEs. The χ^1 and χ^2 angles of Met[1], Phe[4], and Leu[6] could not be defined solely on the basis of the NMR observations ($^3J_{\alpha CH-\beta(\beta')CH}$ coupling constants and NOE contacts), because they were compatible with more than one staggered conformation. However, the preferred side chain orientation for Met[1] and Phe[4] could be selected on the basis of severe side chain to backbone steric repulsions. The Leu[6] side chain conformation could instead be modeled into two plausible conformations by qualitatively combining local steric hindrance and experimental NMR data.

The starting structures were energy minimized using the conjugate gradient method and then subjected to RMD and MD simulations. These steps were performed to solely refine the initial models. The experimental distances, derived from 52 NOEs, were utilized as distance restraints in RMD simulations (see Table 2). The upper and lower bound restraints were calculated with ±10% of the distance obtained from the NOESY spectra. Appropriate *pseudo*atom corrections[49] were applied for $\beta(\beta')$ protons of dap[5] and $\delta(\delta')$ protons of Leu[6]. Both the MD and the RMD simulations were performed *in vacuo* at 300 K. A skewed biharmonic function was used for distance restraining; different decreasing values of the force constant (30, 10, and 5 kcal/mol Å^2) were applied. The equations of motion were solved using the Leapfrog integration algorithm, with a time step of 0.5 fs.[50] The simulation protocol consisted of an equilibration period of 50 ps. In this step the temperature was held constant, at 300 K, by direct scaling of the velocities. The following simulation period of 360 ps was carried out without velocity rescaling since energy conservation was observed, and the average temperature remained essentially constant around the target value of 300 K. A structure was saved every 25 fs during the simulations for analysis. The final averaged structures were then checked for consistency with all observable NOE.

Results

NMR Analysis. Proton resonances were assigned following the standard procedures by the use of homonuclear TOCSY,[36] NOESY,[37] and DQF−COSY[35] experiments (see Table 1). Quantitative information on *inter*proton distances, listed in Table 2, was obtained from analyzing the NOESY spectrum[37] with a mixing time of 300 ms. An examination of all NMR data indicates that, except for the Leu[6] side chain, *cyclo*(Met[1]-asp[2]-Trp[3]-Phe[4]-dap[5]-Leu[6])*cyclo*(2β-5β) adopts only one predominant conformation in CD_3CN. Qualitatively, a type I/I′ β-turn enclosing Met[1]-asp[2] residues is suggested by the presence and by the relative intensities of the NOE connectivities between Met[1]NH and asp[2]NH, and between asp[2]NH and Trp[3]NH (see Table 2).[51] The small $^3J_{NH-\alpha CH}$ coupling constant of Met[1] (5.4 Hz) and the slightly larger $^3J_{NH-\alpha CH}$ of asp[2] (6.5 Hz) are also in line with a type I/I′ β-turn structure. This turn is presumably stabilized by a hydrogen bond between Trp[3]NH and Leu[6]C′O, as indicated by the small temperature coefficient of the amide Trp[3] proton (−1.7 ppb/K). Similarly, the observable NOE connectivities between Phe[4]NH and dap[5]NH and between dap[5]-NH and Leu[6]NH, together with the $^3J_{NH-\alpha CH}$ coupling constant values of Phe[4] (6.6 Hz) and dap[5] (5.9 Hz), are consistent with a type I/I′ β-turn with the Phe[4]-dap[5] segment at the corner positions.[51] A hydrogen bond between Leu[6]NH and Trp[3]C′O can also be hypothesized on the basis of the small temperature coefficient of the amide Leu[6] proton (−0.9 ppb/K). More likely, type I′ β-turns (instead of type I) are present because of (i) the NOE effect asp[2]NH−Met[1]αCH together with the NOE effect Met[1]NH−Met[1]αCH being stronger than asp[2]NH−asp[2]αCH and (ii) the NOE effect dap[5]NH−Phe[4]αCH together with the NOE

(45) *Insight II User Guide,* Vers. 2.3.0; Biosym Technologies: San Diego CA, 1993.
(46) Lifson, S.; Hagler, A. T.; Dauber, P. J. *J. Am. Chem. Soc.* **1979**, *101*, 5111−5121.
(47) Hagler, A. T.; Lifson, S.; Dauber, P. J. *J. Am. Chem. Soc.* **1979**, *101*, 5122−5130.
(48) Hagler, A. T.; Dauber, P. J.; Lifson, S. *J. Am. Chem. Soc.* **1979**, *101*, 5131−5140.
(49) Wuthrich, K.; Billeter, M.; Braun, W. *J. Mol. Biol.* **1983**, *169*, 949−961.
(50) Hockney, R. W. *Methods Comput. Phys.* **1970**, *9*, 136−141.
(51) Perczel, A.; Hollosi, M.; Sandor, P.; Fasman, G. D. *Int. J. Pept. Protein Res.* **1993**, *41*, 223−236.

Table 2. *Inter*Proton Distances Calculated from NOESY Spectra in CD_3CN and Averaged Values during the RMD Simulations[a]

cross-peak	NOESY	RMD^{ttg+}	RMD^{g-g-t}	cross-peak	NOESY	RMD^{ttg+}	RMD^{g-g-t}
Met^{1}NH−asp^{2}NH	2.9	2.8	2.8	Phe^{4}NH−Phe^{4}αCH	2.1	2.3	2.3
Met^{1}NH−Leu^{6}αCH	2.2	2.2	2.2	Phe^{4}αCH− Phe^{4}6H	2.7	2.8	2.8
Met^{1}NH−Met^{1}αCH	2.2	2.3	2.3	Phe$^4\beta$CH− Phe^{4}2H	2.6	2.4	2.4
Met^{1}αCH−Met$^1\beta$CH	2.2	2.4	2.4	Phe$^4\beta'$CH− Phe^{4}6H	2.5	2.6	2.6
Met^{1}αCH−Met$^1\beta'$CH	2.7	3.0	3.0	Phe^{4}αCH− Phe^4_βCH	3.2	3.0	3.1
Met^{1}αCH−Met$^1\gamma$CH	2.5	2.6	2.5	Phe^{4}αCH− Phe^4_β'CH	2.9	2.6	2.6
asp^{2}NH−Trp^{3}NH	2.5	2.6	2.6	dap^{5}NH−Leu^{6}NH	3.1	3.0	2.9
asp^{2}NH−dap$^5\beta$NH	2.5	2.4	2.4	dap^{5}NH−Phe^{4}αCH	2.8	2.6	2.6
asp^{2}NH−Met^{1}αCH	2.8	2.8	2.8	dap$^5\beta$NH−asp$^2\beta$CHproS	2.2	2.2	2.2
asp^{2}NH−asp^{2}αCH	3.2	3.0	3.0	dap^{5}NH−dap^{5}αCH	2.9	3.0	3.0
asp^{2}NH−asp$^2\beta$CHproS	2.6	2.8	2.8	dap^{5}NH−dap$^5\beta\beta'CH_2$	2.4	3.1	3.1
asp^{2}αCH−asp$^2\beta$CHproR	2.4	2.4	2.4	dap$^5\beta$NH−dap$^5\beta\beta'CH_2$	2.1	2.5	2.5
asp^{2}αCH−asp$^2\beta$CHproS	2.4	2.5	2.5	dap^{5}αCH−dap$^5\beta\beta'CH_2$	2.2	2.2	2.3
Trp^{3}NH−Leu^{6}NH	3.0	3.1	3.1	Leu^{6}NH−Leu^{6}αCH	2.9	3.0	3.1
Trp^{3}NH−Trp^{3}αCH	2.9	3.0	3.1	Leu^{6}NH−Leu$^6\beta$CH	2.7	2.7	2.5
Trp^{3}NH−Trp$^3\beta$CHproS	2.5	2.6	2.6	[c]Leu^{6}NH−Leu$^6\beta'$CH	2.7	2.5	3.7
Trp^{3}NH−Trp$^3\beta$CHproR	2.9	3.0	3.0	[b]Leu^{6}NH−Leu$^6\gamma$CH	3.4	4.6	3.2
Trp^{3}4H−Trp^{3}αCH	3.0	2.8	2.8	[c]Leu^{6}αCH−Leu$^6\beta$CH	2.8	2.5	3.1
Trp^{3}4H−Trp$^3\beta$CHproS	3.2	3.9	4.0	Leu^{6}αCH−Leu$^6\beta'$CH	3.0	3.0	2.6
Trp^{3}4H−Trp$^3\beta$CHproR	2.8	2.5	2.5	[b]Leu^{6}αCH−Leu$^6\delta CH_3$	2.7	4.6	3.0
Trp^{3}αCH−Trp$^3\beta$CHproS	2.9	3.1	3.1	[c]Leu^{6}αCH−Leu$^6\delta' CH_3$	2.8	3.0	4.6
Trp^{3}αCH−Trp$^3\beta$CHproR	2.5	2.5	2.5	[c]Leu$^6\beta'$CH−Leu$^6\gamma$CH	2.9	2.6	3.0
Trp^{3}2H−Trp$^3\beta$CHproS	3.1	2.7	2.7	[c]Leu$^6\beta$CH−Leu$^6\delta CH_3$	3.0	3.1	3.8
Trp^{3}2H−Trp$^3\beta$CHproR	3.4	3.8	3.8	[c]Leu$^6\beta$CH−Leu$^6\delta' CH_3$	2.6	2.9	2.8
Phe^{4}NH−dap^{5}NH	2.8	2.8	2.8	Leu$^6\beta'$CH−Leu$^6\delta CH_3$	2.7	2.8	3.0
Phe^{4}NH−Trp^{3}αCH	2.1	2.2	2.2	[c]Leu$^6\beta'$CH−Leu$^6\delta' CH_3$	3.7	3.7	3.0

[a] All values are given in Å. For the upper and lower distance restraint, 10% was added or subtracted. Standard cross-peak: Trp$^3\beta$CHpro*S*−Trp$^3\beta$CHpro*R*, d = 1.78 Å. RMD^{ttg+} and RMD^{g-g-t} indicate the simulations starting from a *trans*, *trans* (*gauche*(−)) and a *gauche*(−), *gauche*(−) (*trans*) Leu^6 side chain conformation, respectively. [b] NOEs omitted in the RMD^{ttg+} simulation (see text). [c] NOEs omitted in the RMD^{g-g-t} simulation (see text).

effect Phe^{4}NH−Phe^{4}αCH being stronger than dap^{5}NH−dap^{5}αCH. $^3J_{NH-\alpha CH}$ coupling constants of Trp^3 (9.8 Hz) and Leu^6 (9.2 Hz) are in agreement with an extended conformation of both residues; the ϕ solution of the Karplus equation is around −120° for both residues.[51,53] Furthermore, the strong NOE effects between Met^{1}NH and Leu^{6}αCH, and Phe^{4}NH and Trp^{3}αCH suggest positive ψ angles for both Trp^3 and Leu^6 residues. The long-range NOE effect between Trp^{3}NH and Leu^{6}NH is also particularly diagnostic for Trp^3 and Leu^6 residues typically hydrogen bonded in an antiparallel β-strand orientation. The χ^1 and χ^2 angles of asp^2 and dap^5 determine the orientation of the lactame bridge. Unambiguous values of $^3J_{\alpha CH-\beta(\beta')CH}$ coupling constants (4.2 Hz) and NH−$\beta(\beta')$CH, and αCH−β-(β')CH cross-peak intensities, allowed us to attribute a *gauche*(−) conformation for the asp^2 χ^1 angle (the calculated population[42,43] for χ^1 would be about 80% for the *gauche*(−) conformer and 3% and 17% for the *gauche*(+) and *trans* populations, respectively). Furthermore, dap$^5\beta$NH-asp^{2}NH NOESY cross-peak intensity indicates an asp^2 χ^2 angle ($C^{\alpha}{}_2-C^{\beta}{}_2-C^{\gamma}{}_2-N^{\beta}{}_5$) of about +90°. Consequently, a unique conformation for dap^5 was derived, with a *gauche*(−) χ^1 angle, and a χ^2 angle ($C^{\alpha}{}_5-C^{\beta}{}_5-N^{\beta}{}_5-C^{\gamma}{}_2$) of about +90°. *Intra*-residue NOESY cross-peaks and $^3J_{\alpha CH-\beta-(\beta')CH}$ coupling constants (10.1 and 5.4 Hz) allowed us also to identify the side chain conformation of Trp^3. The χ^1 angle was set to 180° (the calculated population[42,43] would be about 76% for the *trans* conformer and 18% and 6% for the *gauche*(+) and *gauche*(−) populations, respectively). Moreover, the NOE derived *inter*proton distances between Trp^{3}4H with Trp^{3}αCH and Trp$^3\beta(\beta')$CH indicate a *skew*(−) Trp^3 χ^2 angle. The side chain orientation of Met^1, Phe^4, and Leu^6 were defined in the initial model using both the NMR observations and severe side chain to backbone steric repulsions occurring for some staggered side chain conformations. This is feasible in this particular case because the conformation of the backbone and of asp^2 and dap^5 lactame bridge is unequivocally determined by the numerous and clear NMR observations described up to now. The $^3J_{\alpha CH-\beta(\beta')CH}$ coupling constants of Met^1 (4.3 and 10.1 Hz) indicate either a *trans* or a *gauche*(−) χ^1 angle. However, the *trans* conformation was rejected because of the severe steric repulsion between the Met$^1C^{\gamma}$ and Met^{1}O atoms. This occurs when the ψ angle is of about 30°. In addition, the observed strong NOESY cross-peak Met^{1}αCH−Met$^1\gamma$CH and the absence of a Met^{1}αCH−Met$^1\gamma'$CH NOESY cross-peak was indicative of either a *gauche*(+) or *trans* χ^2 angle. The *trans* isomer was preferred because the combination of a *gauche*(−) χ^1 angle and a *gauche*(+) χ^2 angle would lead the S^{γ} atom to a bumping position with Met^{1}NH (> 0.1 Å van der Waals radii overlap). The $^3J_{\alpha CH-\beta(\beta')CH}$ coupling constants of Phe^4 (2.8 and 11.3 Hz) gave also two possible values of the χ^1 angle: *trans* or *gauche*(−). The *trans* isomer was rejected also in this case because of severe steric repulsions between Phe$^4C^{\gamma}$ and the Phe^{4}O atoms (the ψ angle of Phe^4 is about 30°). The χ^2 angle of Phe^4 was arbitrarily set to the commonly observed value of ±90°. For the Leu^6 side chain, it was not possible to find a single conformation which fits all the experimental data. In fact, the $^3J_{\alpha CH-\beta-(\beta')CH}$ coupling constants of Leu^6 (7.6 Hz) suggested more than one conformer to be appreciably populated. Moreover, the NOE contacts could not be interpreted by a single conformation but only by an averaging between two or more conformations. The *gauche*(+) conformer for the χ^1 angle was discarded because of severe steric repulsions with the Leu^6 side chain and the backbone atoms (this holds true for the ψ angle of Leu^6 between 90 and 270°). The remaining staggered conformations for the χ^1 angle (*trans* and *gauche*(−)) were both considered separately in the subsequent RMD and MD calculations. In addition, the χ^2 angles were set, on the basis of unacceptable steric repulsions, to *trans* (*gauche*(+)), when the χ^1 angle was set to *trans* and to *gauche*(−) (*trans*), when the χ^1

(52) Karplus, M. *J. Chem. Phys.* **1959**, *30*, 11−15.
(53) Bystrov, V. F. *Prog. Magn. Res. Spectrosc.* **1976**, *10*, 41−82.

Table 3. Average Torsion Angles (deg) of *cyclo*(Met[1]-asp[2]-Trp[3]-Phe[4]-dap[5]-Leu[6])*cyclo*(2β-5β) as Obtained from RMD and MD Simulations *in Vacuo* at 300 K

residue	ϕ	ψ	ω	χ^1	$\chi^{2,1}$	$\chi^{2,2}$
(a) RMD^{ttg+} (First Row) and MD^{ttg+} (Middle Row for the Most Populated Conformer and Third Row for the Less Populated Conformer)						
Met[1]	56	34	−169	−58	−177	
	68(8)	−49(14)	−178(9)	−161(10)	−180(14)	
				−63(11)	67(13)	
	57(10)	28(18)	−171(7)	−64(10)	−179(14)	
					71(13)	
asp[2] [a]	81	10	171	−75	89[b]	
	173(16)	26(20)	167(8)	−69(6)	87(10)	
	91(18)	−3(19)	168(7)	−73(6)	84(9)	
Trp[3]	−117	97	−169	−176	−98	
	−131(21)	102(10)	−167(8)	−176(8)	−108(12)	
	−102(20)	96(9)	−171(6)	−176(9)	−105(13)	
Phe[4]	56	42	−168	−61	100	
	57(9)	41(11)	−173(8)	−63(10)	97(14)	
	56(8)	45(10)	−170(7)	−62(9)	98(14)	
dap[5] [a]	73	−5	176	−74	80[c]	
	71(13)	1(14)	170(7)	−72(6)	84(9)	
	74(12)	−13(14)	174(7)	−73(6)	83(9)	
Leu[6]	−99	96	−169	−172	−166	73
	−92(14)	92(10)	−167(7)	−175(9)	−171(10)	68(10)
	−89(15)	94(9)	−169(7)	−174(9)	−170(11)	68(11)
(b) RMD^{g-g-t} (First Row) and MD^{g-g-t} (Middle Row for the Most Populated Conformer and Third Row for the Less Populated Conformer)						
Met[1]	56	34	−170	−58	−176	
	68(8)	−51(14)	−178(9)	−161(10)	64(12)	
	54(9)	40(12)	−172(6)	−156(14)	68(11)	
asp[2] [d]	81	9	170	−75	90[b]	
	178(9)	34(12)	167(8)	−70(6)	87(10)	
	81(12)	−5(19)	169(7)	−74(6)	83(9)	
Trp[3]	−116	98	−170	−176	−98	
	−136(16)	101(10)	−169(6)	−176(8)	−108(13)	
	−100(18)	95(8)	−171(6)	−176(8)	−106(12)	
Phe[4]	56	44	−168	−64	100	
	58(10)	42(11)	−174(9)	−62(9)	98(13)	
	56(8)	45(11)	−169(6)	−61(8)	97(12)	
dap[5] [d]	71	0	177	−73	80[c]	
	70(10)	1(15)	170(7)	−72(6)	85(10)	
	75(12)	−15(15)	175(7)	−73(5)	83(9)	
Leu[6]	−105	96	−168	−75	−73	166
	−92(14)	92(10)	−166(7)	−174(9)	−170(10)	68(11)
	−89(15)	93(8)	−168(6)	−174(9)	−170(10)	68(11)

[a] The $C^{\beta}_2-C^{\gamma}_2-N^{\gamma}_5-C^{\beta}_5$ value from RMD is 163° and those from MD are 181(7)° and −173(7)° for conformers A and B, respectively. [b] $C^{\alpha}_2-C^{\beta}_2-C^{\gamma}_2-N^{\gamma}_5$. [c] $C^{\gamma}_2-N^{\gamma}_5-C^{\beta}_5-C^{\alpha}_5$. [d] The $C^{\beta}_2-C^{\gamma}_2-N^{\gamma}_5-C^{\beta}_5$ value from RMD is −176° and those from MD are 179(7)° and −172(7)° for conformers A and B, respectively.

angle was set to *gauche*(−). All 12 conflicting NOEs involving the Leu[6] side chain protons can now completely be interpreted by taking into account these two fast interconverting Leu[6] side chain conformers. In particular, 10 out of 12 NOEs are consistent with the *trans*, *trans* (*gauche*(−)) χ^1 and χ^2 angles, respectively; five NOEs are, instead, consistent with the *gauche*(−) and *gauche*(−) (*trans*) χ^1 and χ^2 angles, respectively.

Molecular Dynamic Calculations. The large number of *inter*proton correlations (64, 11 of which are main chain to main chain, with 3 NOEs per residue), the low-temperature coefficients of Trp[3] and Leu[6] amide protons, and the ^3J coupling constant values enabled us to build two reasonable initial models for *cyclo*(Met[1]-asp[2]-Trp[3]-Phe[4]-dap[5]-Leu[6])*cyclo*(2β-5β). These two starting models, named *tt*(*g*+) and *g*−*g*−(*t*), differed in the Leu[6] side chain conformation only. The relative conformer populations could not be achieved because of the lack of stereospecific assignment for Leu[6] β,β' protons.[42,43]

These two models were independently refined by RMD calculations *in vacuo* at 300 K. Two NOEs inconsistent with the *tt*(*g*+) conformer, but consistent with the *g*−*g*−(*t*) conformer (indicated with the superscript "b" in Table 2), were omitted from the distance restrain list in the RMD calculations. Analogously, seven NOEs in contradiction to the *g*−*g*−(*t*) conformer, but consistent with the *tt*(*g*+) conformer (indicated with the superscript "c" in Table 2), were not included in the distance restrain list for the refinement of this structure. In summary, a set of 50 and 45 *inter*proton distances, obtained from NOESY spectra in CD_3CN solution, were used in the RMD simulations for *tt*(*g*+) and *g*−*g*−(*t*) conformers, respectively. When decreasing values of the force constant (30, 10, and 5 kcal/mol Å^2) were applied to the distance constraints, substantially similar average structures were observed; the following discussion refers to the conformational parameters obtained with a force constant of 5 kcal/mol Å^2. Table 2 compares the *inter*proton distances obtained from experimental NOEs and from the two RMD simulations; a good agreement between the values can be observed. The RMD simulations on both conformers lead to two average structures of the bicyclic hexapeptide with quite similar backbone torsion angles. It is noteworthy that the assumption of two conformers in fast equilibrium for the Leu[6] side chain yielded a good agreement with the NOE data. The average molecular conformations, along the trajectory of the RMD simulations, are reported in Tables 3 and 4. Figure 1 illustrates a superimposition of the averaged molecular structures of *cyclo*(Met[1]-asp[2]-Trp[3]-Phe[4]-dap[5]-Leu[6])*cyclo*(2β-5β), as obtained from the two RMD simula-

Table 4. *Intra*Molecular Hydrogen Bonds of *cyclo*-(Met[1]-asp[2]-Trp[3]-Phe[4]-dap[5]-Leu[6])*cyclo*(2β-5β)

donor (D)	acceptor (A)	$d_{(D\cdots A)}$ (Å) RMD	$d_{(D\cdots A)}$ (Å) MD conformer A	$d_{(D\cdots A)}$ (Å) MD conformer B
(a) As Obtained from RMD^{ttg+} and from MD^{ttg+} Simulations *in Vacuo* at 300 K				
Trp^{3}HN	Leu^{6}C′O	3.2	3.5	3.2
Leu^{6}HN	Trp^{3}C′O	3.2	3.4	3.3
dap^{5}HN	asp$^2\beta$C′O	3.0	3.0	3.0
Met^{1}HN	dap^{5}C′O	3.6	3.4	3.4
asp^{2}HN	Leu^{6}C′O		2.9	
(b) As Obtained from RMD^{g-g-t} and from MD^{g-g-t} Simulations *in Vacuo* at 300 K				
Trp^{3}HN	Leu^{6}C′O	3.2	3.5	3.3
Leu^{6}HN	Trp^{3}C′O	3.2	3.5	3.3
dap^{5}HN	asp$^2\beta$C′O	3.0	3.0	3.0
Met^{1}HN	dap^{5}C′O	3.7	3.4	3.4
asp^{2}HN	Leu^{6}C′O		2.9	

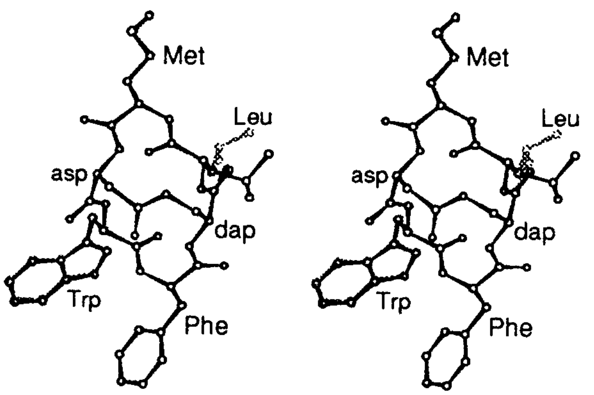

Figure 1. Stereoview of the backbone atoms superimposition of the *tt*(*g*+) and *g*−*g*−(*t*) average molecular structures of *cyclo*(Met[1]-asp[2]-Trp[3]-Phe[4]-dap[5]-Leu[6])*cyclo*(2β-5β), as obtained from RMD simulations (the rmsd is 0.037 Å).

tions. The root-mean-square displacement (rmsd) obtained from the backbone atom superimposition (29 atom pairs) is 0.037 Å.

The energy-minimized average structures of both *tt*(*g*+) and *g*−*g*−(*t*) conformers from the RMD simulations were used as starting structures in two independent MD calculations *in vacuo* at 300 K. These simulations gave average structures quite similar to that obtained from RMD simulations, except for higher molecular motion of the Met^1−asp^2 peptide bond. By the inspection of the plot of ψ Met^1 and ϕ asp^2 vs time during the MD simulations (see Figure 2), it was possible to distinguish, for both *tt*(*g*+) and *g*−*g*−(*t*) conformers, two populations of conformers, named A and B. The ψ_1, ϕ_2 average torsion angles are as follows: (i) $\psi_1 = -49°$, $\phi_2 = 173°$ and $\psi_1 = -51°$, $\phi_2 = 178°$ for conformer A, derived from the *tt*(*g*+) and *g*−*g*−(*t*) starting models, respectively; (ii) $\psi_1 = 28°$, $\phi_2 = 91°$ and $\psi_1 = 40°$, $\phi_2 = 81°$ for conformer B, derived from the *tt*(*g*+) and *g*−*g*−(*t*) starting models, respectively. The peptide bond Met^1−asp^2 flips between two orientations. The peptide bond planes are rotated of about 60°. One of these conformations (A) is the most frequently observed (63% and 80% of the *tt*(*g*+) and *g*−*g*−(*t*) simulation time, respectively) along the trajectory of the MDs. The less populated conformers (B) are quite similar to the average structures obtained from RMDs. The conformational parameters of both conformers are reported in Tables 3 and 4. By an inspection of Table 3, it can be noted that the *trans*, *trans* (*gauche*(+)) starting conformation of the Leu^6 side chain was retained during the MD simulations, for both the A and B conformations. In contrast, in the *g*−*g*−(*t*) isomer, the

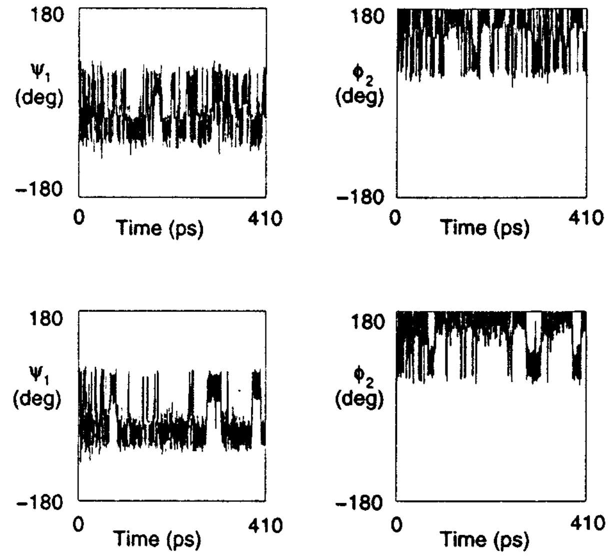

Figure 2. Plot of the ψ angle of Met^1 (left) and ϕ angle of asp^2 (right) vs time during the MD simulation, for the *tt*(*g*+) conformer (upper) and *g*−*g*−(*t*) conformer (lower). It is possible to distinguish two conformational families in both the simulations.

χ^1 and χ^2 torsion angles changed from *gauche*(−), *gauche*(−) (*trans*) to *trans*, *trans* (*gauche*(+)), which seems to be the preferred Leu^6 side chain orientation. The rmsd obtained from the backbone atom superimposition of the average RMD model with the A and B MD isomers are 0.51 and 0.13 Å, respectively, for both the *tt*(*g*+) and *g*−*g*−(*t*) models.

The superimpositions of the two average conformations, obtained from the MD$^{tt(g+)}$ (upper panel) and MD$^{g-g-(t)}$ (lower panel) are reported in Figure 3 (rmsd = 0.45 and 0.54 Å, respectively).

Discussion

RMD calculations indicate that the structure of MEN10701 is characterized in CD_3CN solution by (1) a type I′ β-turn with Met^1-asp^2 at the corner positions of the turn, stabilized by a Trp^{3}NH- - -Leu^{6}C′O hydrogen bond and (2) a type I′ β-turn with Phe^4-dap^5 at the corner positions stabilized by a Leu^{6}NH- - -Trp^{3}C′O hydrogen bond. The structure of MEN10701 is the first observation, to the best of our knowledge, of a cyclic hexapeptide characterized by two type I′ β-turns, which are enclosing heterochiral sequences (Met^1-asp^2 and Phe^4-dap^5 segments). The conformational behavior of MEN10701 well agrees with the high propensity of heterochiral sequences to be accommodated into the $i + 1$ and $i + 2$ positions of β-turns. However, cyclic hexapeptide structures, with amino acids of different chirality, such as DDLDDL or LLDLLD, unlike MEN10701, strongly prefer type II or II′ β-turned structures.[54−59] Rotation of both Met^1−asp^2 and Phe^4−dap^5 peptide bonds would lead to two type II β-turns, but the C′O groups of Met^1 and Phe^4 would be oriented toward the center of the molecule. Severe repulsions of the carbonyls with atoms of the lactame bridge would result. The lactame bridge also participates to the *intra*molecular hydrogen bond network, because the asp$^2\beta$C′O is at a short distance to dap^{5}NH of the main cycle (see Table 4).

Trp^3 and Leu^6 face each other with an arrangement similar to that of hydrogen bonded residues in an antiparallel β-sheet orientation. Trp^3 adopts a β-extended conformation (ϕ, ψ = −117, 97° and −116, 98° in the *tt*(*g*+) and *g*−*g*−(*t*), respec-

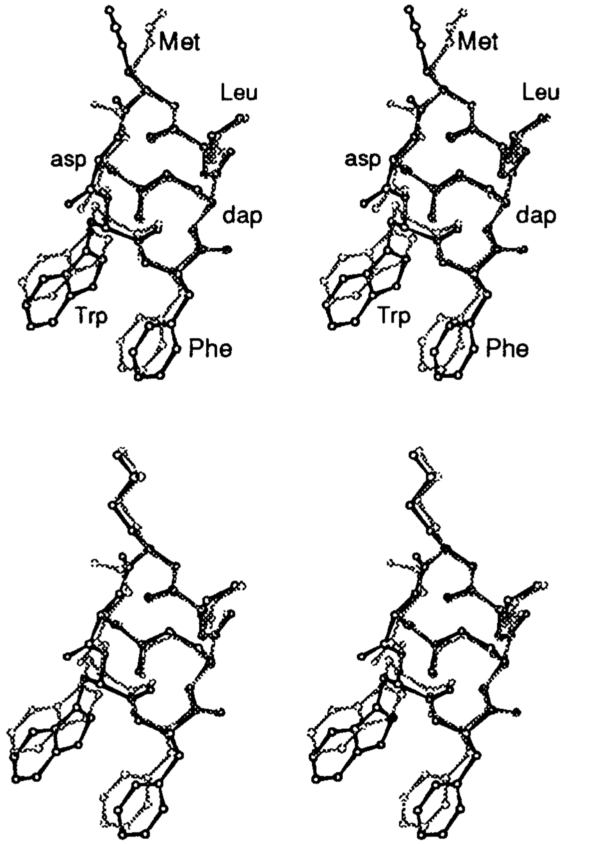

Figure 3. Stereoview of the backbone atoms superimposition of the two A and B average molecular conformations of *cyclo*(Met^1-asp^2-Trp^3-Phe^4-dap^5-Leu^6)*cyclo*(2β-5β), obtained from the MD *tt*(g+) (upper panel) and $g-g-(t)$ (lower panel) simulations (the rmsds are 0.45 and 0.54 Å, respectively).

tively). Leu^6 is partially folded into a γ^i-turned conformation (ϕ, ψ = −99, 96° and −105, 96° in the *tt*(g+) and $g-g-(t)$, respectively), which is stabilized by a weak $i + 2 \rightarrow i$ hydrogen-bond interaction between Met^{1}NH and dap^{5}C′O. However, the NH of Met^1 is pointing outward the molecular core, and thus it is solvent exposed. This observation may account for the high-temperature coefficient observed for the Met^1 NH.

The MD simulations revealed the presence of a second conformational family, in both the *tt*(g+) and $g-g-(t)$ conformers, which is slightly different from that obtained from RMD calculations. A distorted γ-turn around the Met^1 residue, stabilized by a Leu^{6}C′O−asp^{2}NH hydrogen bond, is also observed. In this conformation, rarely observed for L-amino acid residues, five of the seven NHs are *intra*molecularly hydrogen bonded. This may account for the stabilization of the axial γ-turn. However, it should be pointed out that simulations *in vacuo* and in the presence of solvent can lead to different average structures.[60−63] In fact, it is well-documented that simulations carried out *in vacuo* tend to result in artificial, more compact structures, with an overabundance of hydrogen bonds.[60−63] To overcome these effects and in an attempt to mimic the electrostatic interactions with the solvent, we have also performed the MD simulations using the dielectric constant appropriate for the solvent.[64] The resulting average conformations, for both the *tt*(g+) and $g-g-(t)$ isomers, were identical to those obtained from RMD simulations *in vacuo*, where the influence of the solvent is mimicked by the experimental restraints used in the calculations. Moreover, it should be noted that the absence of solvent in the MD calculations do not distort the overall conformation of the molecule, and the average conformations resulting from *in vacuo* MD calculations agree well with those derived from NMR experimental data and RMD simulations.

In summary, RMD and MD calculations indicate that MEN10701 is characterized in CD_3CN solution by a global shape similar to a "*football*" and quite different from the flat rectangular shape observed in solution and in the solid state for MEN10627 and for *cyclo*(Phe^1-Asp^2-Trp^3-Phe^4-Dap^5-Trp^6)-*cyclo*(2β-5β). The bridge residues Asp^2 and Dap^5 are located in the i and $i + 3$ positions of two β-turns for the homochiral analogue, while in the heterochiral sequence, as in MEN10701, the bridge residues, which are of opposite configuration, both occupy the $i + 2$ position of two β-turns. This shift of β-turn corner positions determines a completely different molecular shape in MEN10701 respect to MEN10627.

Despite our expectations, the uncoercible bicyclic structure of MEN10627 is thus dramatically coerced into a novel conformation, by the replacement of the lactame bridge forming units (Asp^2 and Dap^5) with residues of opposite chirality.

We have recently shown that the homochiral peptide sequence *cyclo*(Aaa^1-Asp^2-Aaa^3-Aaa^4-Dap^5-Aaa^6)*cyclo*(2β-5β) represents a rigid molecular scaffold for engineering type I and type II β-turn structures, where Aaa^3-Aaa^4 and Aaa^6-Aaa^1 correspond to α-amino acid residues which occupy the $i + 1$ and $i + 2$ positions of a type I β-turn and a type II β-turn, respectively. We propose here that the heterochiral sequence *cyclo*(Aaa^1-asp^2-Aaa^3-Aaa^4-dap^5-Aaa^6)*cyclo*(2β-5β), which contains D-Asp and D-Dap as the lactame-bridge-forming residues at positions 2 and 5 of the sequence, can be used as a novel rigid molecular scaffold for engineering type I′ β-turns where Aaa^3, Aaa,^{4} and Aaa,^{6} or Aaa,^{6} Aaa^1, and Aaa^3 correspond to α-amino acid residues which occupy the i, $i + 1$, and $i + 3$ positions of a type I′ β-turn. This structure can be added to the repertoire of rigid β-turn scaffolds for the design of bioactive molecules that require turned motifs to elicit potency and specificity. However, the use as scaffolds implies that the conformation observed for this specific molecule will be maintained regardless of the L-amino acid type incorporated into this peptide; such a generalization deserves more examples to be considered as proven.

When analyzing the molecular conformation of MEN10701, it was quite surprising to discover that the relative positions of the Phe^4, Trp^3, Leu^6 and Met^1 Cα and Cβ atoms are very close to those of the Cα and Cβ atoms of residues i to $i + 4$ and $i + 1$ to $i + 5$ of an "ideal" α-helix.[65] The C^{α} atom distances

(54) Toniolo, C. *CRC Crit. Rev. Biochem.* **1980**, 1−44 and references therein.
(55) Varughese, K. I.; Kartha, G.; Kopple, K. D. *J. Am. Chem. Soc.* **1981**, *103*, 3310−3313.
(56) Brown, J. N.; Yang, C. H. *J. Am. Chem. Soc*. **1979**, *101*, 445−449.
(57) Brown, J. N.; Teller, R. G. *J. Am. Chem. Soc*. **1976**, *98*, 7565−7569.
(58) Kostansek, E. C.; Lipscomb, W. N.; Thiessen, W. E. *J. Am. Chem. Soc*. **1979**, *101*, 834−837.
(59) Flippen-Anderson, J. L. *Pept., Struct. Biol. Funct., Proc. Am. Pept. Symp., 6th* **1979**, 145−148.
(60) Mierke, D. F.; Kessler, H. *Biopolymers* **1993**, *3*, 1003−1017.
(61) Kessler, H.; Bats, J. W.; Griesinger, C.; Koll, S.; Will, M.; Wagner, K. *J. Am. Chem. Soc.* **1988**, *110*, 1133−1049.
(62) Levitt, M.; Saron, R. *Proc. Natl. Acad. Sci. U.S.A.* **1988**, *85*, 7577−7561.
(63) Kurz, M.; Mierke, D. F.; Kessler, H. *Angew. Chem., Int. Ed. Engl.* **1992**, *31*, 210−212.
(64) Wendoloski, J. J.; Matthew, J. B. *Proteins Struct. Funct. Genet.* **1989**, *5*, 313−321.
(65) Perutz, M. F. *Nature* **1951**, *167*, 1053−1054.

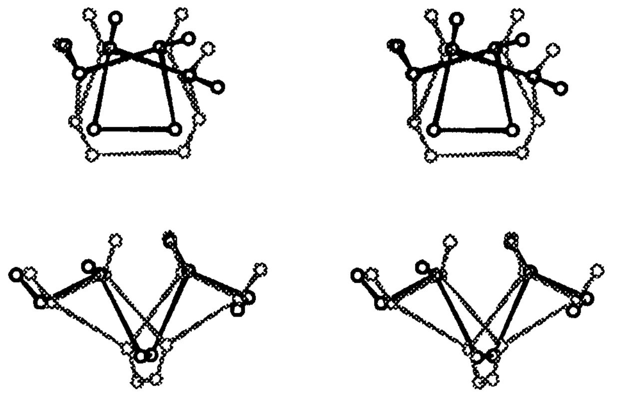

Figure 4. Stereoview of the superimposition of the C^{α} atoms for the residues 1, 2, 5 and 6 of an "ideal" α-helix (thick line), with the C^{α} atoms of the residues 4, 3, 6, and 1 of MEN10701.

Trp^3-Met^1 and Phe^4-Leu^6 are about 5.7 Å, as typically found for residues *i* and $i + 4$ of a α-helix. The bicyclic structure of MEN10701 represents a highly constrained small peptide that can also be used as scaffold for mimicking one face of a α-helix. To the best of our knowledge, there is no example reported so far in the literature of a molecular tool that can be used for this purpose. Figure 4 describes in a stereoview the superimposition of the C^{α} atoms for the residues 1, 2, 5, and 6 of an ideal α-helix with the C^{α} atoms of the residues 4, 3, 6, and 1 of MEN10701. The root-mean-square deviation for the superimposition of these atoms is only 0.24 Å.

In conclusion, the conformational behavior of MEN10701 indicates that this molecule exhibit a quite unique structure which can be used to mimic both type I′ β-turns or small stretches of α-helical structures.

Acknowledgment. This work was supported by Menarini Pharmaceuticals.

JA9643329